NUMERICAL SIMULATION OF LOW-REYNOLDS NUMBER, TWO-DIMENSIONAL UNSTEADY FLOW ABOUT ROTATING CIRCULAR CYLINDERS

L. Baranyi

PhD, Department of Fluid and Heat Engineering, University of Miskolc, Miskolc, Hungary

This paper presents a finite difference solution of the 2-D, unsteady incompressible Navier-Stokes equations for laminar flow about a rotating cylinder placed in an otherwise uniform flow. The governing equations are written a non-inertial system fixed to the rotating cylinder. The orthogonal transformation provides a fine grid near the wall and a coarse field far from the cylinder. Time derivatives are handled by forward differences, convective terms by a third order upwind difference, other space derivatives are by high order central differences. The variation of lift and drag coefficients with time are presented for different values of rotation parameter α. The variation of time mean and root-mean-square (r.m.s.) values with α are also shown for two meshes.

1 Introduction

It has been known for a long time that a spinning cylinder will develop large lift forces when placed in a uniform stream; this is the so called Magnus effect. The first person who used this device on a large scale for ship propulsion was Flettner, and the device was named after him. Rotating cylinder is also a means of boundary layer or circulation control. By moving part of the wall it is possible to eliminate the formation of the boundary layer by attempting to eliminate the velocity difference between the wall and flow, which is the very source of boundary layer formation. Using a rotating cylinder at the leading edge (see Lewis & Arain (1991)) or at the trailing edge (see Tennant *et al*. (1976)) of an aerofoil, flow separation can be prevented resulting in high lift and low drag. Hyung *et al*. (1995) carried out experimental tests on the flow past a rotating cylinder in uniform shear flow. Chew *et al*. (1995) and Cheng *et al*. (1997) developed a hybrid vortex scheme in which the vorticity transport equation is broken into two fractional steps: pure diffusion and inviscid convection are handled separately. They applied their methods for computation of flows around fixed and rotating cylinders.

There are different methods available for the computation of flows past fixed or oscillating cylinder, Karniadakis & Triantafyllou (1989), Menighini & Bearman (1995), Baranyi & Shirakashi (1999a) and Baranyi *et al*. (1999b). In the latter papers the authors

present a computational method, based on a finite difference solution of the Navier-Stokes equations and a pressure Poisson equation written in a non-inertial system fixed to the oscillating cylinder. This method is extended here for the computation of the flow past a rotating cylinder placed into a uniform stream. Computational results are presented for lift and drag coefficients. Based on computational results the author attempts to evaluate the efficiency of the Magnus effect in creating lift.

2 Governing Equations

The primitive variable formulation is used for the solution of the problem. The governing equations are: two components of the non-conservation form of the Navier-Stokes equations and the equation of continuity. These equations which contain only dimensionless quantities are written in the non-inertial system fixed to the rotating cylinder, referred to as relative system from now on. The equations have the following forms

$$\frac{\partial u}{\partial t}+u\frac{\partial u}{\partial x}+v\frac{\partial u}{\partial y}=-\frac{\partial p}{\partial x}+\frac{1}{Re}\left(\frac{\partial^2 u}{\partial x^2}+\frac{\partial^2 u}{\partial y^2}\right)+4\alpha v+4\alpha^2 x+2\frac{d\alpha}{d t}y; \tag{1}$$

$$\frac{\partial v}{\partial t}+u\frac{\partial v}{\partial x}+v\frac{\partial v}{\partial y}=-\frac{\partial p}{\partial y}+\frac{1}{Re}\left(\frac{\partial^2 v}{\partial x^2}+\frac{\partial^2 v}{\partial y^2}\right)-4\alpha u+4\alpha^2 y-2\frac{d\alpha}{d t}x; \tag{2}$$

$$\Theta=\frac{\partial u}{\partial x}+\frac{\partial v}{\partial y}=0. \tag{3}$$

In these equations all quantities are non-dimensionalized by the combinations of a reference length $L=d$, a reference velocity U, the density ρ and kinematic viscosity υ. Here d is the diameter of the cylinder and U is the upstream velocity. Consequently the Reynolds number Re is defined as $Re=Ud/\nu$. In the equations above x, y are Cartesian co-ordinates, u, v are the x, y components of velocity in the relative system fixed to the cylinder, p is the pressure, Θ is dilation, t is time, α is the cylinder rotation parameter defined as the ratio of the peripheral velocity and freestream velocity

$$\alpha=\frac{\Omega d}{2U}. \tag{4}$$

Here Ω is the angular velocity of the cylinder. It is positive when the direction of rotation is counter clockwise.

Although theoretically equations (1) – (3) are applicable for the determination of the three unknowns *u*, *v* and *p*, according to Harlow & Welch (1965) it is advisable to use a separate equation for the determination of pressure *p*. Taking the divergence of the Navier-Stokes equations (1) and (2) yields a Poisson equation for pressure

$$\frac{\partial^2 p}{\partial x^2}+\frac{\partial^2 p}{\partial y^2}=2\left[\frac{\partial u}{\partial x}\frac{\partial v}{\partial y}-\frac{\partial u}{\partial y}\frac{\partial v}{\partial x}\right]-\frac{\partial \Theta}{\partial t}+4\,\alpha\,\omega+8\alpha^2 \tag{5}$$

where

$$\omega=\frac{\partial v}{\partial x}-\frac{\partial u}{\partial y} \tag{6}$$

is the vorticity. Governing equations (1) – (3) and (5) are valid for flows around cylinders rotating with variable angular velocity ($\alpha=\alpha(t)$), with constant angular velocity $(\alpha=const)$, and also for stationary cylinder ($\alpha=0$). Although strictly the dilation $\Theta=0$ by continuity, still it is advisable to retain its partial derivative with respect to time in equation (5) to avoid instability, Harlow & Welch (1965). Equations (1), (2) and (5) will be solved while the continuity equation (3) is satisfied at every time step. The body force due to gravity is included in the pressure term.

2.1 Boundary and initial conditions

The basic equations are written for the incompressible fluid in a non-inertial system fixed to the rotating cylinder. The physical domain defined by dimensionless inner and outer radii R_1 and R_2, is shown on the left-hand side (LHS) of Figure 1. In the relative system it looks as if the parallel flow were rotating with non-dimensional angular velocity $-\Omega$. At dimensionless time *t* the freestream velocity *U* includes an angle of

$$\vartheta=\Omega\,t \tag{7}$$

with the *x* axis (see the figure). Due to lack of space, the way quantities are nondimensionalized will not be explained here, we only refer to Baranyi & Shirakashi (1999a). The relationship between rotational parameter α defined by equation (4) and dimensionless Ω is $\Omega=2\alpha$.

Before considering the boundary conditions (BCs) let us write the relationship in an arbitrary point of the physical domain between velocities *u*, *v* in the relative system and absolute velocities u_a, v_a measured in the inertial system. Taking into account basic kinematics the relationship between these velocities runs as follows

$$u_a = u\cos\vartheta + v\sin\vartheta - 2\alpha R\sin\varphi; \tag{8}$$

$$v_a = v\cos\vartheta - u\sin\vartheta - 2\alpha R\cos\varphi \tag{9}$$

where R is the dimensionless distance from the origin, ϑ is the angle shown in Figure 1, related to cylinder rotation, φ is polar angle measured in the relative system; it is zero in the direction of the positive x axis and is increasing in clockwise direction. Let us investigate now the boundary conditions.

On the surface of the cylinder (R_1) (See Figure 1):

Velocity: no-slip condition

$$u = v = 0. \tag{10}$$

Pressure:

$$\frac{\partial p}{\partial n} = \frac{1}{Re}\nabla^2 v_n - 2\alpha^2. \tag{11}$$

where n refers to components in the direction of the outer normal. Equation (8) is obtained from Navier-Stokes equations (1) and (2).

Far from the cylinder (R_2):

Velocity: uniform absolute flow

$$u = \cos(2\alpha t) - 2\alpha R_2 \sin\varphi; \tag{12}$$

$$v = -\sin(2\alpha t) - 2\alpha R_2 \cos\varphi. \tag{13}$$

These time-dependent BCs were obtained from equations (8) and (9) assuming uniform flow at R_2 in the inertial system, and equation (7) was also taken into account.

Pressure:

$$\frac{\partial p}{\partial n} \cong 0. \tag{14}$$

It is to be noted that the assumption of uniform flow in the far field region is reasonable except for the narrow wake since the outer boundary of the computational domain is very far from the cylinder.

Initial conditions are obtained from the assumption that the cylinder is started abruptly at $t = 0$. Substituting $\vartheta = 0$, $u = U = 1$ and $v = 0$ into equations (8) and (9) yields initial conditions for velocity

$$u = 1 - 2\alpha R\sin\varphi; \tag{15}$$

$$v = -2\alpha R\cos\varphi, \tag{16}$$

and pressure p is considered to be constant at $t = 0$.

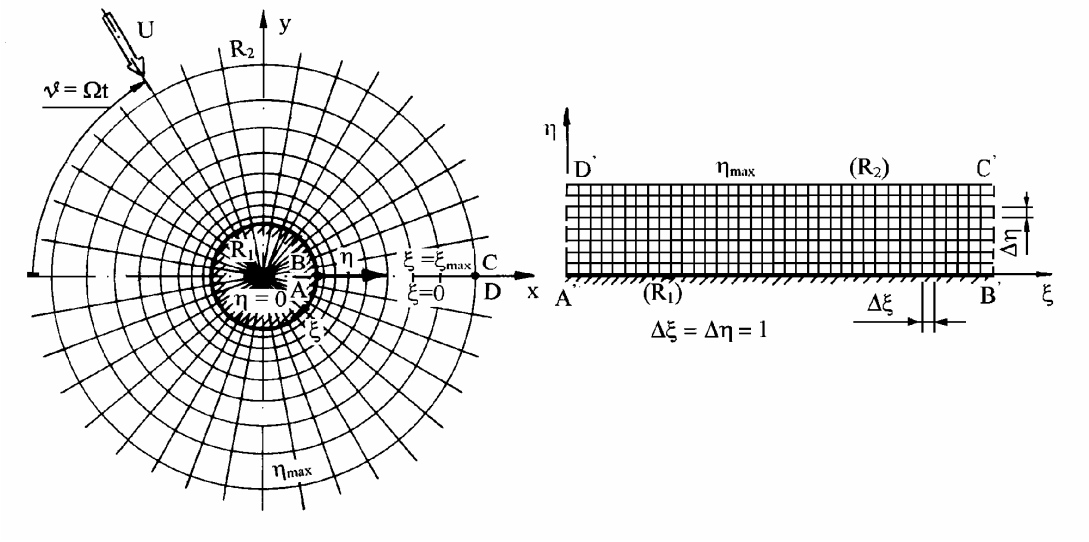

Figure 1 Physical and computational planes

3 Transformation from Physical Plane to Computational Plane

We use boundary-fitted co-ordinates on the physical plane since boundary conditions can only be represented accurately when the boundary is such that it coincides with some coordinate line. This physical domain shown on the LHS of Figure 1 is transformed onto a rectangular domain - computational plane - which can be seen in the right-hand side (RHS) of the figure. A unique and single-valued relationship between the co-ordinates on the computational domain (ξ, η, τ) and the physical co-ordinates (x, y, t) can be written as (see Baranyi *et al.* (1999b))

$$\begin{aligned} x(\xi,\eta) &= R(\eta)\cos\left[g(\xi)\right]; \\ y(\xi,\eta) &= -R(\eta)\sin\left[g(\xi)\right]; \\ t &= \tau \end{aligned} \tag{17}$$

where the dimensionless radius

$$R(\eta) = R_1 \exp\left[f(\eta)\right]. \tag{18}$$

This choice of the structure of the mapping function automatically assures that the obtained grid is orthogonal on the physical plane for arbitrary functions $f(\eta)$ and $g(\xi)$.

By choosing the mapping functions properly a very fine grid can be obtained in the vicinity of the cylinder and a coarse grid far from the body. Even linear functions for $f(\eta)$

and $g(\xi)$ can provide this feature. Transformations (17) and (18) are unique and single-valued only for non-vanishing Jacobian J

$$J = \frac{\partial x}{\partial \xi}\frac{\partial y}{\partial \eta} - \frac{\partial x}{\partial \eta}\frac{\partial y}{\partial \xi}. \tag{19}$$

The x and y components of the Navier-Stokes equations will be transformed as follows

$$\frac{\partial u}{\partial \tau} + \frac{1}{J}\left(u\frac{\partial y}{\partial \eta} - v\frac{\partial x}{\partial \eta}\right)\frac{\partial u}{\partial \xi} + \frac{1}{J}\left(v\frac{\partial x}{\partial \xi} - u\frac{\partial y}{\partial \xi}\right)\frac{\partial u}{\partial \eta} = -\frac{1}{J}\left(\frac{\partial y}{\partial \eta}\frac{\partial p}{\partial \xi} - \frac{\partial y}{\partial \xi}\frac{\partial p}{\partial \eta}\right) +$$

$$+ \frac{1}{Re\,J^2}\left(g_{22}\frac{\partial^2 u}{\partial \xi^2} + g_{11}\frac{\partial^2 u}{\partial \eta^2} + \varphi\frac{\partial u}{\partial \xi} + \sigma\frac{\partial u}{\partial \eta}\right) + 4\alpha v + 4\alpha^2 x + 2\frac{d\alpha}{d t}y; \tag{20}$$

$$\frac{\partial v}{\partial \tau} + \frac{1}{J}\left(u\frac{\partial y}{\partial \eta} - v\frac{\partial x}{\partial \eta}\right)\frac{\partial v}{\partial \xi} + \frac{1}{J}\left(v\frac{\partial x}{\partial \xi} - u\frac{\partial y}{\partial \xi}\right)\frac{\partial v}{\partial \eta} = -\frac{1}{J}\left(\frac{\partial x}{\partial \xi}\frac{\partial p}{\partial \eta} - \frac{\partial x}{\partial \eta}\frac{\partial p}{\partial \xi}\right) +$$

$$+ \frac{1}{Re\,J^2}\left(g_{22}\frac{\partial^2 v}{\partial \xi^2} + g_{11}\frac{\partial^2 v}{\partial \eta^2} + \varphi\frac{\partial v}{\partial \xi} + \sigma\frac{\partial v}{\partial \eta}\right) - 4\alpha u + 4\alpha^2 y - 2\frac{d\alpha}{d t}x \tag{21}$$

The dilation Θ transforms as

$$\Theta = \frac{1}{J}\left(\frac{\partial y}{\partial \eta}\frac{\partial u}{\partial \xi} - \frac{\partial y}{\partial \xi}\frac{\partial u}{\partial \eta} + \frac{\partial x}{\partial \xi}\frac{\partial v}{\partial \eta} - \frac{\partial x}{\partial \eta}\frac{\partial v}{\partial \xi}\right) = 0. \tag{22}$$

The Poisson equation for pressure will have the form

$$g_{22}\frac{\partial^2 p}{\partial \xi^2} + g_{11}\frac{\partial^2 p}{\partial \eta^2} + \varphi\frac{\partial p}{\partial \xi} + \sigma\frac{\partial p}{\partial \eta} = 2J\left(\frac{\partial u}{\partial \xi}\frac{\partial v}{\partial \eta} - \frac{\partial u}{\partial \eta}\frac{\partial v}{\partial \xi}\right) - J^2\frac{\partial \Theta}{\partial \tau} +$$

$$+ 4\alpha J\left(\frac{\partial y}{\partial \eta}\frac{\partial v}{\partial \xi} - \frac{\partial y}{\partial \xi}\frac{\partial v}{\partial \eta} - \frac{\partial x}{\partial \xi}\frac{\partial u}{\partial \eta} + \frac{\partial x}{\partial \eta}\frac{\partial u}{\partial \xi}\right) + 8\alpha^2 J^2. \tag{23}$$

Boundary conditions for pressure will be transformed as

$$R = R_1: \quad \frac{\partial p}{\partial \eta} = \frac{1}{ReJ^2}\left[\frac{\partial x}{\partial \eta}\left(g_{11}\frac{\partial^2 u}{\partial \eta^2} + \sigma\frac{\partial u}{\partial \eta}\right) + \frac{\partial y}{\partial \eta}\left(g_{11}\frac{\partial^2 v}{\partial \eta^2} + \sigma\frac{\partial v}{\partial \eta}\right)\right] - 2\alpha^2; \tag{24}$$

$$R = R_2: \quad \frac{\partial p}{\partial \eta} \cong 0. \tag{25}$$

In equations (20) - (24) variables g_{11}, g_{22}, φ and σ are defined as follows

$$g_{11} = \left(\frac{\partial x}{\partial \xi}\right)^2 + \left(\frac{\partial y}{\partial \xi}\right)^2; \tag{26}$$

$$g_{22} = \left(\frac{\partial x}{\partial \eta}\right)^2 + \left(\frac{\partial y}{\partial \eta}\right)^2; \tag{27}$$

$$\varphi = \frac{1}{J}\left[\frac{\partial x}{\partial \eta}\left(g_{22}\frac{\partial^2 y}{\partial \xi^2} + g_{11}\frac{\partial^2 y}{\partial \eta^2}\right) - \frac{\partial y}{\partial \eta}\left(g_{22}\frac{\partial^2 x}{\partial \xi^2} + g_{11}\frac{\partial^2 x}{\partial \eta^2}\right)\right]; \tag{28}$$

$$\sigma = \frac{1}{J}\left[\frac{\partial y}{\partial \xi}\left(g_{22}\frac{\partial^2 x}{\partial \xi^2} + g_{11}\frac{\partial^2 x}{\partial \eta^2}\right) - \frac{\partial x}{\partial \xi}\left(g_{22}\frac{\partial^2 y}{\partial \xi^2} + g_{11}\frac{\partial^2 y}{\partial \eta^2}\right)\right]. \tag{29}$$

In these equations g_{11} and g_{22} are elements of the metric tensor. Because of the structure of transformation (17) and (18) the grid is always orthogonal. Hence the off-diagonal metric tensor elements $g_{12} = g_{21} = 0$. That is also the reason why the mixed second derivatives are missing from the equations above.

Since the mapping is given by elementary functions, all of the metric parameters and co-ordinate derivatives can be computed from closed forms. In this way the numerical differentiation of co-ordinates subjected to numerical errors can be avoided.

It can be shown by using equations (17) - (19) and (28) that when $g(\xi)$ is a linear function then $\varphi = 0$. If *f* is a linear function of η then $\sigma = 0$ too, as can be proved by using equations (17) - (19) and (29). In these cases our equations can be simplified further, and the grid aspect ratio will become constant. By choosing the number of grid points in directions ξ η properly, this constant can be set to unity resulting in conformal transformation.

4 Discussions and Sample Calculations

The computational code developed for the solution of the flow about fixed and oscillating cylinders (see Baranyi & Shirakashi (1999a)) was modified and extended in order that it should be able to tackle this new problem. The transformed governing equations are solved by the finite difference method. The time derivatives in the Navier-Stokes equations (20) and (21) are approximated by forward differences. Fourth order central difference scheme is used for the diffusion terms and pressure derivatives. The widely used modified third order upwind scheme proposed by Kawamura (1984) proved to be successful in handling the convective terms in the Navier-Stokes equations.

The equations of motion are integrated explicitly giving the velocity distribution at every time step. In the knowledge of the velocity distribution in an arbitrary time step, the pressure is calculated from equation (22) by using the successive over-relaxation method (SOR) while the continuity constraint (22) is also satisfied. The pressure on the cylinder

surface is calculated by the third order formula derived from the Taylor series at every time step.

The computational grids used are 145x79 or 241x131 O-meshes. These numbers of grid points were chosen to assure conformal property of the transformation. The diameter of the outer boundary of the computational domain is *30 d.* Dimensionless time steps used were *0.001* and *0.0005*.

Computations were carried out for flows about cylinders rotating with different angular velocities and with *Re = 180.* The effect of rotation parameter α on the lift and drag coefficients was investigated for $0 \le \alpha \le 1.5$ for meshes characterized by 141x79 and 241x131 grid points. Figure 2 shows the variation of lift coefficient C_L, skin friction lift coefficient C_{Lf}, drag coefficients C_D and C_{Df} with dimensionless time, for $\alpha = 0;\ 0.5;\ 1;\ 1.5,$ and for 241x13 mesh. Having a glance at these figures we can see that only small parts of the lift and drag coefficient are due to friction; larger parts are due to pressure. The top part of the figure shows coefficients for fixed cylinder ($\alpha = 0$). In this case the drag coefficients oscillate twice as many as the lift coefficients during a fixed time interval. In case of $\alpha = 0.5$ a second dominant frequency component appears in the drag coefficient. By increasing α further all of the signals show regular fluctuations with constant amplitudes, and the frequency of oscillation for lift and drag will become roughly identical in contrast with fixed cylinder. By applying FFT for the oscillating signals it was found that the change in the vortex shedding frequency, or Strouhal number can be neglected over the investigated α domain.

Computations were carried out for the 145x79 mesh for different α values too. On the other hand time mean values and root-mean-square (*r.m.s.*) values were evaluated for both meshes. Figure 3 shows the mean values for lift and drag coefficients against α for the two meshes and a remarkably good agreement was obtained. It was found that the drag coefficient is slightly decreasing in contrast with the results of Chew *et al.* (1995) who experienced a slight increase in C_D for increasing α. It can be seen in the figure that the absolute value of the lift coefficient increases almost linearly with α. It is known or can be derived easily that for frictionless ideal fluid-flow around a rotating cylinder the lift coefficient C_{Lid} is also a linear function of α, and can be written as follows

$$C_{Lid} = -2\pi\alpha .$$

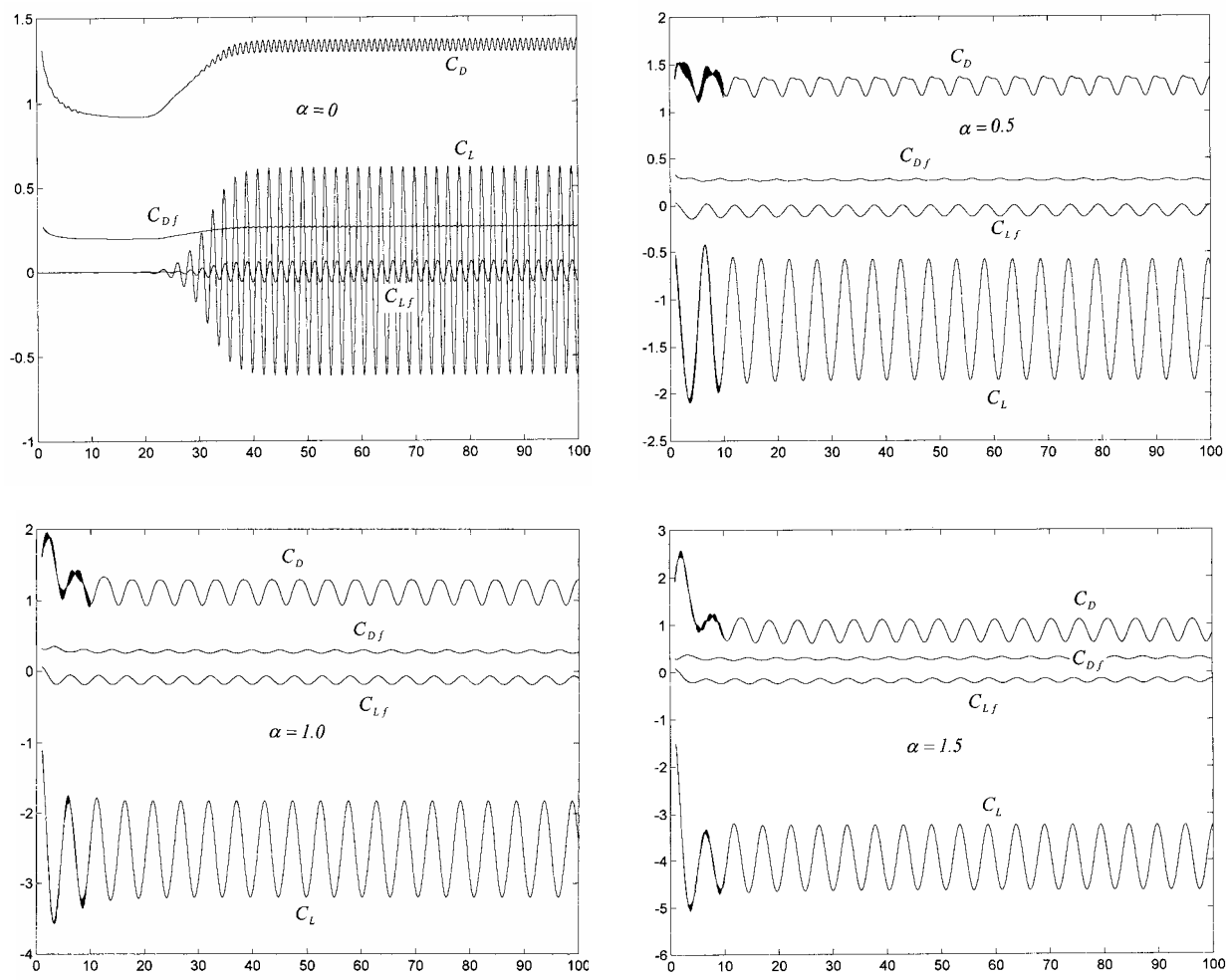

Figure 2 The variation of lift and drag coefficients with α and time

By comparing this relationship with the results in Figure 3 one can say that at this *Re* number and in the investigated α domain the real lift is just about *40 %* of the one predicted by the Magnus effect for ideal fluid.

Figure 4 shows the variation of the *r.m.s.* values of lift and drag coefficients with α for the two meshes mentioned earlier. Having a glance at the figure one can see that while the *r.m.s.* values of the drag coefficient agree very well over a wide range of α domain, the *r.m.s.* values for the lift coefficients for the two meshes differ from each other over the whole α range. The accurate prediction of $C_{L\,r.m.s.}$ requires the application of a dense mesh. It looks like that the accurate prediction of the *r.m.s.* values of the lift coefficient means a severe test of the computational method not only in the case of the fixed or oscillating but for rotating

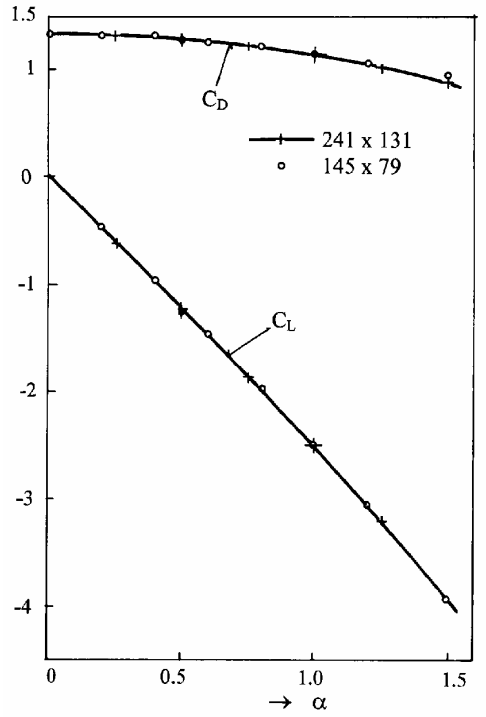

Figure 3 Time-mean values of lift and drag coefficients vs rotational parameter α

cylinders as well. For the computations carried out the angular velocity of rotation was constant so far. We are going to investigate the case when $\alpha = \alpha(t)$ in future.

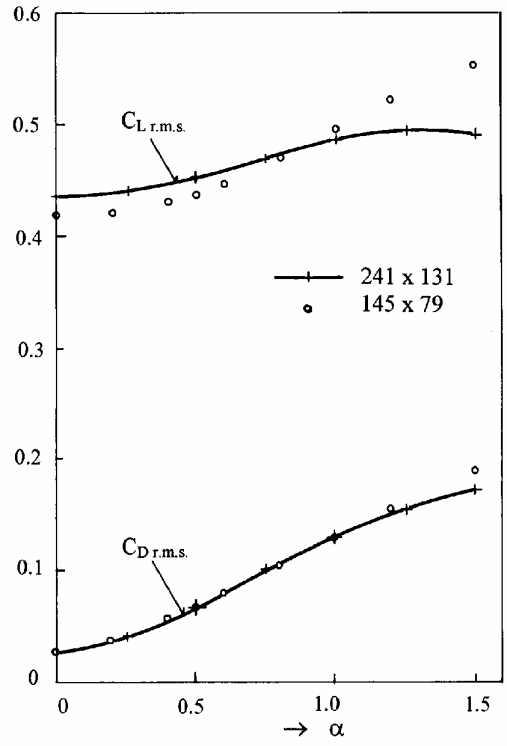

Figure 4 Root-mean-square values of lift and drag coefficients vs rotational parameter α

5 Concluding Remarks

The finite difference method worked out mainly by the present author has been extended and adapted for the numerical simulation of unsteady, laminar incompressible fluid flow about rotating circular cylinders placed in otherwise uniform flows. Primitive variable formulation is used, and equations are derived in a non-inertial system fixed to the cylinder. By using boundary fitted co-ordinates, interpolation of the boundary conditions becomes unnecessary. The choice of a grid fixed to the moving cylinder eliminates the need for interpolation of the initial values at every time step. An orthogonal transformation is used to map the physical plane to the computational one, and the grid density can be controlled. Time derivatives are approximated by forward differences, space derivatives by fourth order central differences except for the convective terms for which a third order modified scheme was used Kawamura (1984). Velocity values are obtained by integrating the Navier-Stokes equations explicitly, and SOR method is used for the determination of the pressure distribution at every time step. The vortex shedding frequency is obtained by applying the FFT for the computed oscillating signals.

Computations have been carried out for different angular velocity or rotation parameter (α) values for two different meshes. Time mean values for lift and drag coefficients agree well with each other for the two meshes but the root-mean-square value of the lift coefficient requires the denser mesh. It seems that the accurate prediction of this quantity is a severe test of the method for not only fixed and oscillating cylinders but for rotating ones too.

References

BARANYI, L. & SHIRAKASHI, M. 1999a Numerical solution for laminar unsteady flow about fixed and oscillating cylinders. *Journal of Computer Assisted Mechanics and Engineering Sciences*, Warsaw, Poland, (accepted for publication), 1-15.

BARANYI, L., SHIRAKASHI, M., & KÓSA, GY. 1999b Computation of two-dimensional laminar unsteady flow past fixed and oscillating cylinders. *Proceedings of the 11th Conference on Fluid and Heat Machinery and Equipment*, Budapest, 1999, (accepted for publication).

CHEW, Y.T., CHENG, M., & LUO, S.C. 1995 A numerical study of flow past a rotating cylinder using a hybrid vortex scheme. *Journal of Fluid Mechanics*, **299**, 35-71.

CHENG, M., CHEW, Y.T., & LUO, S.C. 1997 A hybrid vortex method for flows over a bluff body. *Int. Journal for Numerical Methods in Fluids*, **24**, 253-274.

HARLOW, F.H., & WELCH, J.E. 1965 Numerical Calculation of Time-Dependent Viscous Incompressible Flow of Fluid with Free Surface. *Physics of Fluids*, **8**, 2182-2189.

HYUNG, J.S., CHONG, K.C., & JAE, M.H. 1995 Experimental Study of Uniform Shear Flow Past a Rotating Cylinder. *Journal of Fluids Engineering*, **117**, 62-67.

KARNIADAKIS, G.E., & TRIANTAFYLLOU, G.S. 1989 Frequency Selection and Asymptotic States in Laminar Wakes, *Journal of Fluid Mechanics*, **199**, 441-469.

KAWAMURA, T. 1984 Computation of High Reynolds Number Flow around a Circular Cylinder with Surface Roughness, *Proceedings of the 22nd Aerospace Sciences Meeting*, Reno, Nevada, AIAA-84-0340, 1-11.

LEWIS, R.I, & ARAIN, A.A. 1991 Vortex Dynamics Modelling of a Rotating Cylinder for Aerofoil Lift Control. *Proceedings of the 9th Conference on Fluid Machinery*, Academic Press, Budapest, 256-265.

MENEGHINI, J.R., & BEARMAN, P.W. 1995 Numerical Simulation of High Amplitude Oscillatory Flow About a Circular Cylinder. *Journal of Fluids and Structures*, 435-455.

TENNANT, J.S., JOHNSON, W.S., & KROTHAPALLI, A. 1976 Rotating Cylinder for Circulation Control on an Airfoil. *Journal of Hydronautics*, **10**, 102-105.